Application of thermal methods in the studies of potential pozzolanic reactivity of attapulgite and sepiolite

G. Malata[1] · E. Tkaczewska[1]

Abstract

Aim of study was to verify the effect of temperature on the pozzolanic reactivity of thermally activated attapulgite and sepiolite samples. Activation temperatures were selected: 650, 700 and 750 °C for attapulgite and 800, 825 and 850 °C for sepiolite. Content of pozzolanic reactive SiO_2 and Al_2O_3 after thermal treatment and the amount of $Ca(OH)_2$ consumed in the pozzolanic reaction were measured. It should be noted that a higher activation temperature improves the reactivity of attapulgite and sepiolite. The upper limit for the increase in the pozzolanic reactivity of these materials is the formation of enstatite and the deactivation of silica. In addition to reactive decomposition products, series of minerals formed in the reactions of attapulgite and sepiolite with impurities present in them are also observed.

Keywords Attapulgite · Sepiolite · DTA/TG/DTG · Thermal activation · Pozzolanic reactivity · Compressive strength

Introduction

The term 'pozzolanic reactivity' refers to siliceous-aluminous materials and is defined as a chemical reaction between reactive SiO_2 and Al_2O_3 presented in these materials (the fraction of SiO_2 and Al_2O_3 contained in the glassy constituent in them) and calcium hydroxide in the presence of water to form C–S–H and C–A–H phases that possessed cementitious (hydraulic) properties [1].

The most popular materials used because of their pozzolanic properties are, for example, siliceous fly ashes from the process of bituminous coal dust combustion in furnaces of power and heat and power generating stations in the temperature range of 1200-1400°C. Thanks to this property, which causes complex chemical reactions in the cement paste, the hardened cement mortar structure is filled with additional products that are able to seal and strengthen it [1–4]. However, the time of initiation of the pozzolanic reaction of fly ash is delayed until the release of calcium hydroxide crystals as a product of hydration of

C$_3$S (after a relatively short period of cement hydration) [5] and C$_2$S (after a relatively long period). Slow pozzolanic reaction rate of fly ash (slower than the hydration of pure Portland cement) leads to low strength and slow rate of strength development of cement with fly ashes at early ages; additional amounts of C–S–H and C–A–H phases from the pozzolanic reaction are formed after a long time (after 90 days or later) which improve cement strength [4, 6–9]. Studies [10–13] show that the finer fraction of siliceous fly ashes reveals improved pozzolanic reactivity.

According to the Kyoto Protocol to the United Nations Framework Convention on Climate Change (UNFCCC), adopted in Kyoto on December 11, 1997, the reduction of CO_2 emissions from the coal-fired power plants is realized by substituting coal fuel with sustainably produced biomass. This results in variable properties of fly ashes from coal and biomass combustion [10–15], a consequence of which is the lower pozzolanic reactivity of coal-biomass fly ashes and the slower development of the strength of cement mortar that contains them with time of hydration [12, 27, 28].

The reduction of CO_2 emissions from the cement manufacturing process is realized by substituting Portland cement clinker with waste materials (including through greater uptake of blended cements). In power and heat and power generating stations, if the fuel feed for boiler contains greater than approximately 10% biomass, the resulted fly ash

✉ G. Malata
gmalata@agh.edu.pl

1   Department of Building Materials Technology, Faculty
     of Materials Science and Ceramics, AGH University
     of Krakow, al. Adama Mickiewicza 30, 30-059 Kraków,
     Poland

quality impact can be significant enough to affect utilization in cement applications.

The use of metakaolin as an artificial pozzolan for cement mortar has received considerable interest in recent years. The benefit of using metakaolin is manifested by enhancing the strength of cement mortar, particularly during early age. This very early strength enhancement is due to a combination of the filler effect and accelerated cement hydration in the presence of metakaolin. Studies [15] show that the substitution of 10 mass% of CEM I 52.5R by metakaolin causes a decrease in the early compressive strength, but this reduction is not significant and after 28 days, the strength of this cement blend is similar to that of CEM I 52.5R. This phenomenon is easily explained by the pozzolanic effect, which always delays in time. In the case of metakaolin, this time is relatively short compared to that of fly ashes and is about a month. The grinding of metakaolin to a higher Blaine specific area affects its pozzolanic reactivity [16]. However, metakaolin is more expensive material than Portland cement, although its processing involves moderately low temperatures and its overall production cost is significantly less than that of Portland cement.

Due to artificial pozzolans, in the form of supplementary cementitious materials used, added as a partial replacement for Portland cement clinker in cement mixes, the fresh and hardened properties of cement-based building materials are improved [21–23], new pozzolanic materials are sought, for example thermally activated magnesium silicates such as attapulgite ($Mg_5Si_8O_{20}(OH)_2 \cdot 4H_2O$) and sepiolite ($Mg_4Si_6O_{15}(OH)_2 \cdot 8H_2O$). The use of attapulgite as s supplementary cementing material is mentioned in the articles [17–22]. The influence of sepiolite on the hydration and mechanical properties of Portland cement has been reported in [23].

For thermally activated attapulgite, until now studies have primarily focused on the compressive strength of cement blends [20, 22, 24], including the effect of the curing temperature [19]. The progress of hydration of cement mixture with an addition of activated attapulgite was evaluated as content of non-evaporable (chemically combined) water [20–22], content of reactive SiO_2 [21] and content of free CaO [22]. Shi et al. [20] and Kh Al-Noaimi [22] found that the reactivity of attapulgite is not as good as that of fly ash, but it can be used as a replacement for cement. Zhang et al. [21] showed that thermal activation improves the reactivity of attapulgite by generating a greater amount of reactive SiO_2, resulting in more additional hydrates produced that increase the strength of cement mortar.

In the case of thermally activated sepiolite, Canbaz and Eryilmaz [23] presented only the influence of thermally activated sepiolite on the strength of lime mortar; the workability of lime mortar is decreased proportionally to the sepiolite content. A higher content of sepiolite means

that the greater amount of water is necessary to obtain cement paste of standard consistency, a consequence of which is the reduction in strength.

The publications [20–22, 24] and [23] indicate the effective use of attapulgite and sepiolite (respectively) as a pozzolanic additive, but do not allow one to point out the optimal activation temperature or the appropriate dose of these materials to cement.

The aim of this study is to verify the relationship between the thermal activation temperature of attapulgite and sepiolite and the pozzolanic reactivity of these materials. This relationship is very important from the point of view of the strength of cement and lime mortars modified with thermal activated attapulgite or sepiolite. The attempts were made to study the role and to indicate the estimated values of these two parameters combined with additional evaluation and critical analysis of the pozzolanicity of attapulgite and sepiolite testing methods.

Materials and methods

Materials

The materials used were ordinary Portland cement types of CEM I 32.5R and CEM I 42.5R supplied by one of the Polish cement companies and high-purity commercial magnesium silicate clays such as attapulgite and sepiolite.

Preparation of thermally activated attapulgite and sepiolite samples

The commercial attapulgite and sepiolite samples were heated in an electric furnace at temperatures of:

- 650, 700 or 750 °C for attapulgite (at temperatures at which dehydroxylation of attapulgite has already occurred),
- 800, 825 or 850 °C for sepiolite (temperature of 850 °C corresponds to the decomposition of sepiolite and the beginning of crystallization of enstatite).

After the temperature was reached, the samples were kept in a furnace for one hour. The activated attapulgite samples were denoted: A650—temperature of 650 °C, A700—temperature of 700 °C and A750—temperature of 750 °C. For the activated sepiolite samples, the symbols were: S800—temperature of 800 °C, S825—temperature of 825 °C and S850—temperature of 850 °C.

Methods

Chemical composition of materials

The loss on ignition (LOI) of cements CEM I 32.5R and CEM I 42.5R was determined according to the method described in the PN-EN 196-2:2013 standard [25]. Loss on ignition was calculated by heating cement samples in separate porcelain crucibles to a constant mass in a furnace at a temperature of 1100 °C in an oxidizing atmosphere. The chemical oxide compositions (CaO, SiO_2, Al_2O_3, Fe_2O_3, MgO, Na_2O, K_2O and SO_3) of the cements were determined using methods described in the PN-EN 196-2:2013 standard [25].

In the case of the attapulgite and sepiolite samples, the chemical composition (SiO_2, Al_2O_3, Fe_2O_3, CaO, MgO, Na_2O, K_2O, TiO_2, P_2O_5 and F-fluorine) was tested by X-ray fluorescence analysis (XRF) using a WD-XRF Axios Max spectrometer with a Rh 4 kW PANalytical lamp.

Phase composition of materials

The phase compositions of CEM I 32.5R and CEM I 42.5R cements were calculated using the Bogue method [26]. However, it should be noted that the Bogue method gives only the theoretical (potential) phase composition of these cements based on the calculations from their chemical analysis.

The identification of phases in attapulgite and sepiolite samples was carried out by means of the X-ray diffraction (XRD) technique using a Philips X'Pert Pro MD diffractometer (Cu $K_{\alpha1}$ line monochromatized with a Ge(111) monochromator). Standard Bragg–Brentano geometry with a θ–2θ setup was applied (0.008° step size and 5°–90° 2θ range).

Thermal analysis (DTA/TG/DTG) of attapulgite and sepiolite samples

The thermal decomposition of the attapulgite and sepiolite samples was investigated in an OD 102 thermoanalyzer in air atmosphere. The samples were heated to 1100 °C at heating rate of 0.1 °C/min^{-1}. Endothermic and exothermic peaks corresponding to phase transitions are presented in the DTA curves. The mass losses on the thermogravimetric (TG) curves related to these effects were determined.

Pozzolanic properties of thermally activated attapulgite and sepiolite samples

The pozzolanic properties of thermally activated attapulgite and sepiolite were tested using the chemical method. The content of pozzolanic reactive components (SiO_2 and also Al_2O_3) in thermally activated attapulgite and sepiolite was determined as well as the consumption of calcium hydroxide by these materials was analyzed.

Determination of reactive SiO_2 and Al_2O_3 according to the ASTM C379-65 standard

Using the ASTM C379-65 standard [27], it was possible to determine the contents of reactive SiO_2 and Al_2O_3 in thermally activated attapulgite and sepiolite samples. Reactive SiO_2 and Al_2O_3 were the fractions of SiO_2 and Al_2O_3 that were soluble with a 1 M sodium hydroxide solution (NaOH).

Determination of $Ca(OH)_2$ consumption by attapulgite and sepiolite samples according to the modified Chapelle test

The Chapelle test according to the NF P18-513 standard [28] is one of the direct methods to determine pozzolanic reactivity based on calcium hydroxide consumption. This direct methodology carried out in an aqueous lime-attapulgite or lime-sepiolite system, for one hour at temperature of 90 °C with continuous stirring, allows the quantification of $Ca(OH)_2$ fixed by attapulgite and sepiolite, respectively.

$Ca(OH)_2$ consumed by thermally activated attapulgite and sepiolite (PAA and PAS indexes, respectively) was calculated according to the equation:

$$PAA/PAS = \frac{V_1 - V_2}{V_1} \cdot \frac{74}{56} \cdot 1000$$

where

PAA/PAS—pozzolanic activity of attapulgite and sepiolite, respectively, in milligrams of $Ca(OH)_2$ fixed by 1 g of these materials,

V_1—volume of 0.1 N hydrochloric acid necessary to titrate 25 mL of the final solution obtained without tested materials (blank test), in milliliters,

V_2—volume of 0.1 N hydrochloric acid necessary to titrate 25 mL of the final solution obtained with the tested materials, in milliliters.

Determination of the amount of products formed in the $Ca(OH)_2$-attapulgite(or sepiolite)-water system according to DTA/TG/DTG analysis

For the experiment, mixtures of activated attapulgite (or activated sepiolite), $Ca(OH)_2$ and water in a proportion of 1:3:4 were prepared. The A750 and S850 samples were selected for this study and the pastes with their addition were named, respectively, CH-A750 and CH-S850. The mixtures were stored in tightly closed containers for 28 and 90 days at a temperature of 80 °C. After that, the DTA/TG/DTG

analysis was performed. TG losses were determined in the following temperature ranges:

- 0–250 °C—dehydration of hydrates,
- 250–550 °C—dehydroxylation of $Ca(OH)_2$ (with the maximum rate at 505 °C),
- 550–850 °C—decarbonization of $CaCO_3$.

Results and discussion

Chemical compositions of materials

The results of the chemical analysis of CEM I 32.5R and CEM I 42.5R cements are shown in Table 1. The loss on ignition in both cements does not exceed the acceptable 5 mass% content according to the requirements given in PN-EN 197-1:2012 standard [29]. Additionally, the sulfate content (as SO_3) is below the 4 mass% limit.

The chemical composition of commercial (non-heat treated) magnesium silicate clays used in the experiment, such as attapulgite and sepiolite, is presented in Table 2.

As can be seen in Table 2, the MgO content in attapulgite is 10.67 mass% and is lower by more than two times compared to sepiolite. The contents of Al_2O_3 and Fe_2O_3 in attapulgite are 12.10 and 3.93 mass%, respectively, while those in sepiolite are 5.26 and 1.60 mass%, respectively (the decrease in the content of Al_2O_3 and Fe_2O_3 in sepiolite is more than twice). The share of CaO dominates in the chemical composition of attapulgite and sepiolite. The CaO content is slightly smaller in sepiolite than in attapulgite.

Table 1 Chemical composition of CEM I 32.5R and CEM I 42.5R cements

Chemical component	Method	Content/mass%	
		CEM I 32.5R	CEM I 42.5R
LOI[a]	By the PN-EN 196-2:2013 standard [25]	3.51	2.71
CaO		63.69	64.79
SiO$_2$		19.15	21.85
Al$_2$O$_3$		4.81	3.70
Fe$_2$O$_3$		3.14	0.94
MgO		1.76	1.70
Na$_2$O		0.30	0.38
K$_2$O		0.77	0.92
SO$_3$		2.71	3.01
Na$_2$O$_e$[b]		0.81	0.99
CaO$_{free}$	By the ethylene glycol methodology [31]	1.81	1.80

[a]Loss on ignition determined at temperature of 1100 °C

[b]Sodium equivalent: mass% $Na_2O_e = Na_2O + 0.658 \cdot K_2O$

Table 2 Chemical composition of non-heat treated attapulgite and sepiolite samples by X-ray fluorescence analysis (XRF)

Chemical component	Content/mass%	
	Attapulgite	Sepiolite
SiO$_2$	62.738	61.302
Al$_2$O$_3$	12.101	5.258
Fe$_2$O$_3$	3.932	1.596
CaO	4.597	3.042
MgO	10.974	24.106
Na$_2$O	0.081	0.284
K$_2$O	0.870	1.042
TiO$_2$	0.552	0.207
P$_2$O$_5$	1.111	0.110
F	0.376	0.461

Na_2O, K_2O, TiO_2 and P_2O_5 appear as minor components. The results of chemical composition agree with the data [30].

Phase composition of materials

The potential phase compositions of the CEM I 32.5R and CEM I 42.5R cements based on the Bogue equations [26] are given in Table 3. Their main phases are C_3S (alite) and C_2S (belite), and the rest are C_3A, C_4AF and $CaSO_4$. For CEM I 42.5R cement, the C_3S content is 61.80 mass% and is lower by approximately 8% compared to that of CEM I 32.5R cement, while the C_2S content is 16.02 mass% and is three times higher. The C_3A content in CEM I 42.5R cement is 8.21 mass% and is higher by approximately 10% as compared to CEM I 32.5R cement. For cement CEM I 42.5R, the C_4AF content is 2.86 mass%, while in CEM I 32.5R it is 9.55 mass%. The phase compositions of two Portland cements used correspond to data from the literature [1, 32, 33].

The XRD patterns of commercial (non-heat treated) attapulgite and sepiolite samples are presented in Figs. 1 and 2, respectively. On XRD pattern of attapulgite, in

Table 3 Potential phase composition of CEM I 32.5R and CEM I 42.5R cements based on the Bogue equations [26]

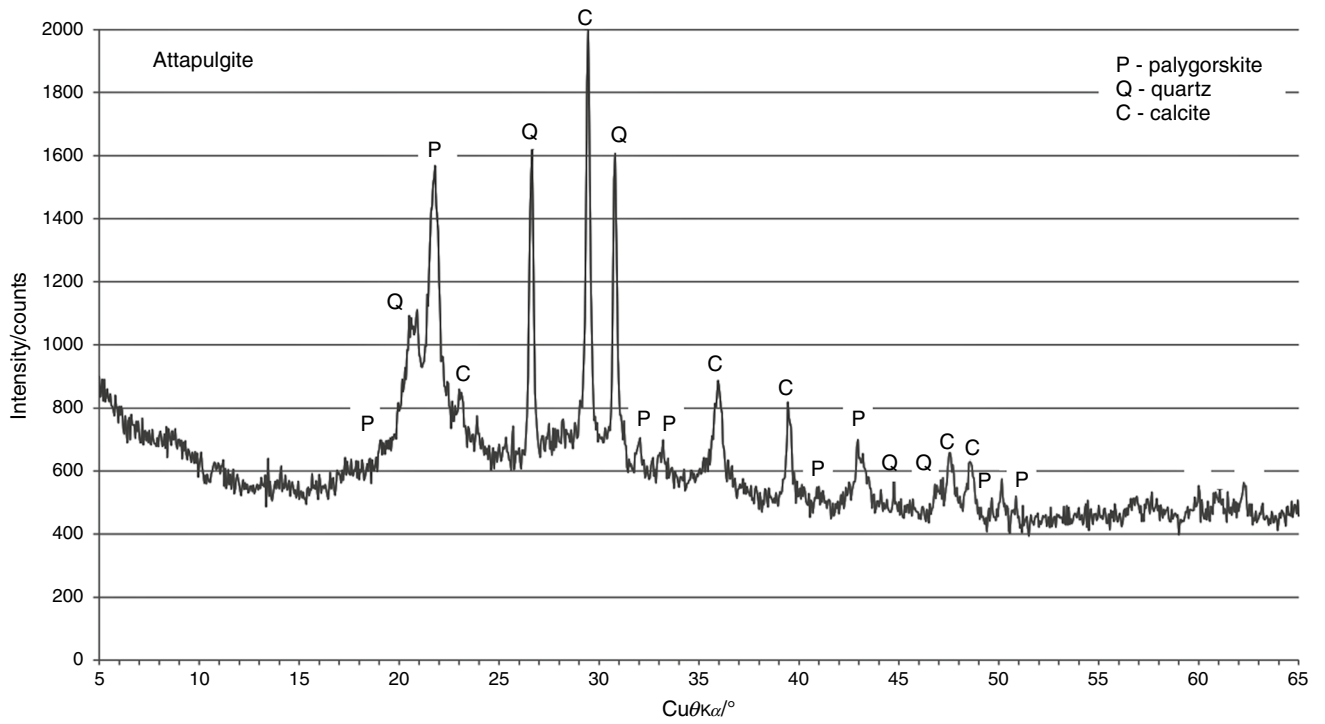| Phase	Content/mass%	
	CEM I 32.5R	CEM I 42.5R
C$_3$S	67.52	61.80
C$_2$S	3.97	16.02
Silicates	71.49	77.82
C$_3$A	7.43	8.21
C$_4$AF	9.55	2.86
Aluminates	16.98	11.07
CaSO$_4$	4.88	5.12

Fig. 1 XRD pattern of commercial (non-heat treated) attapulgite
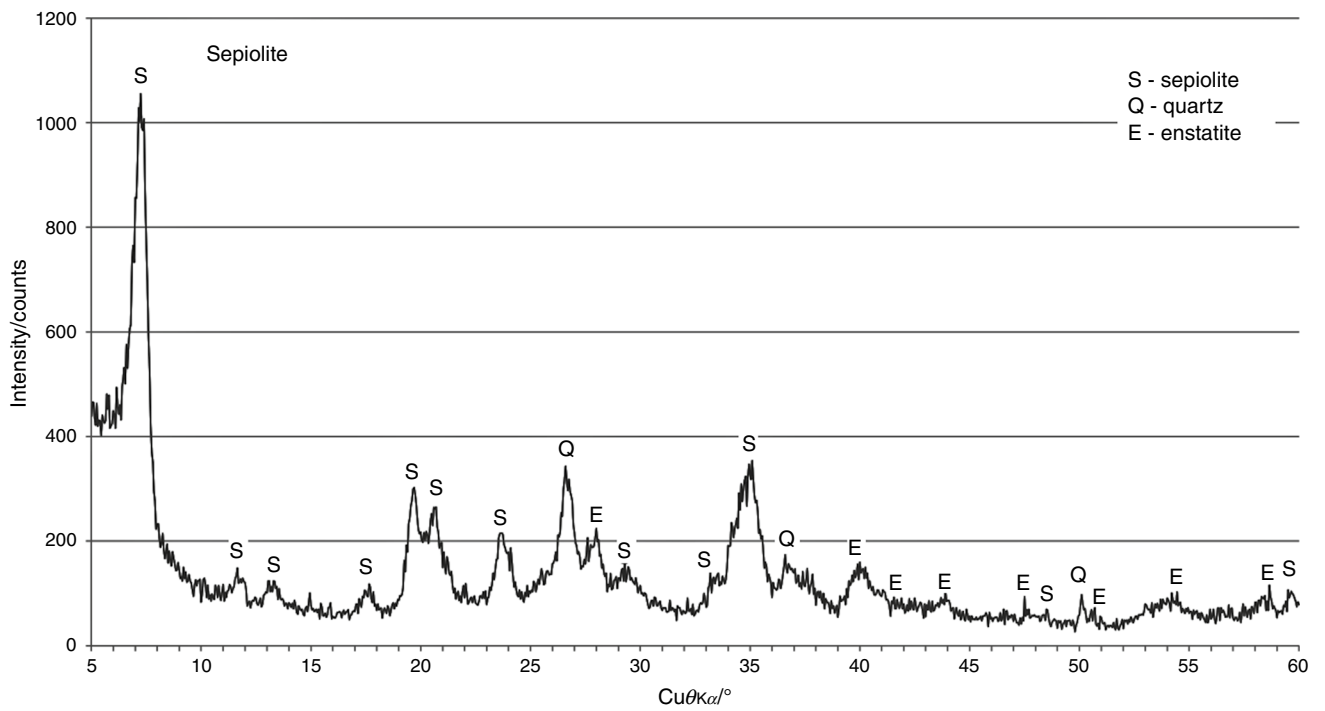
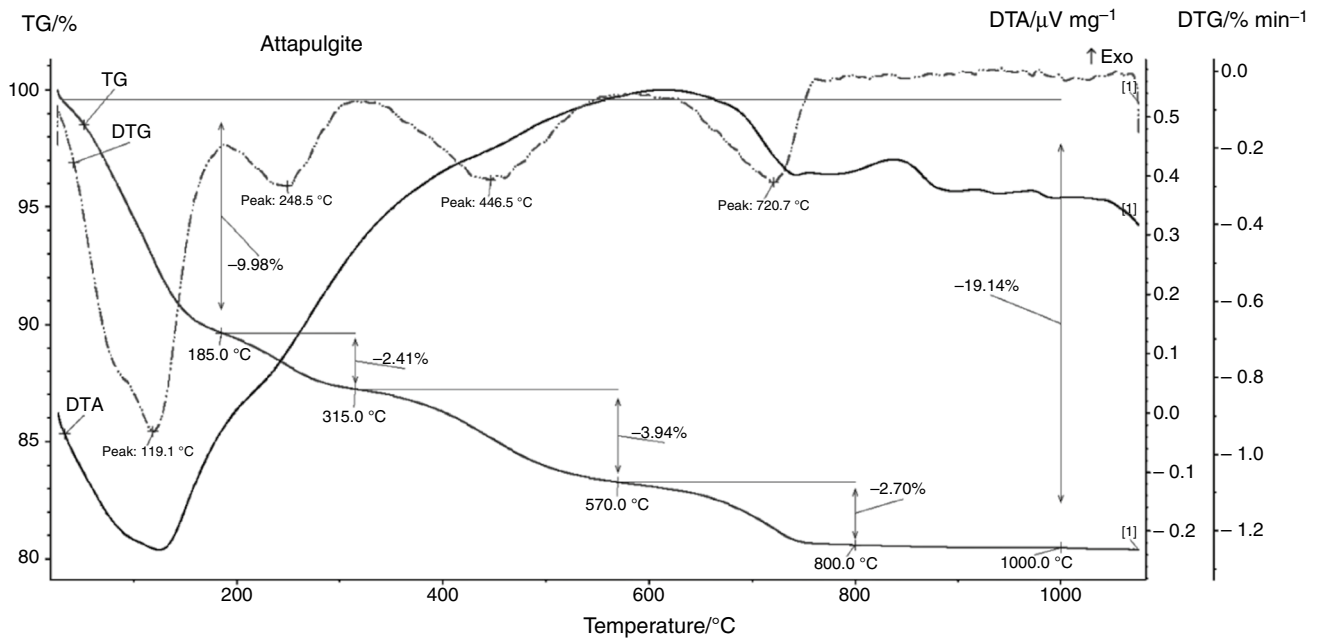**Fig. 2** XRD pattern of commercial (non-heat treated) sepiolite

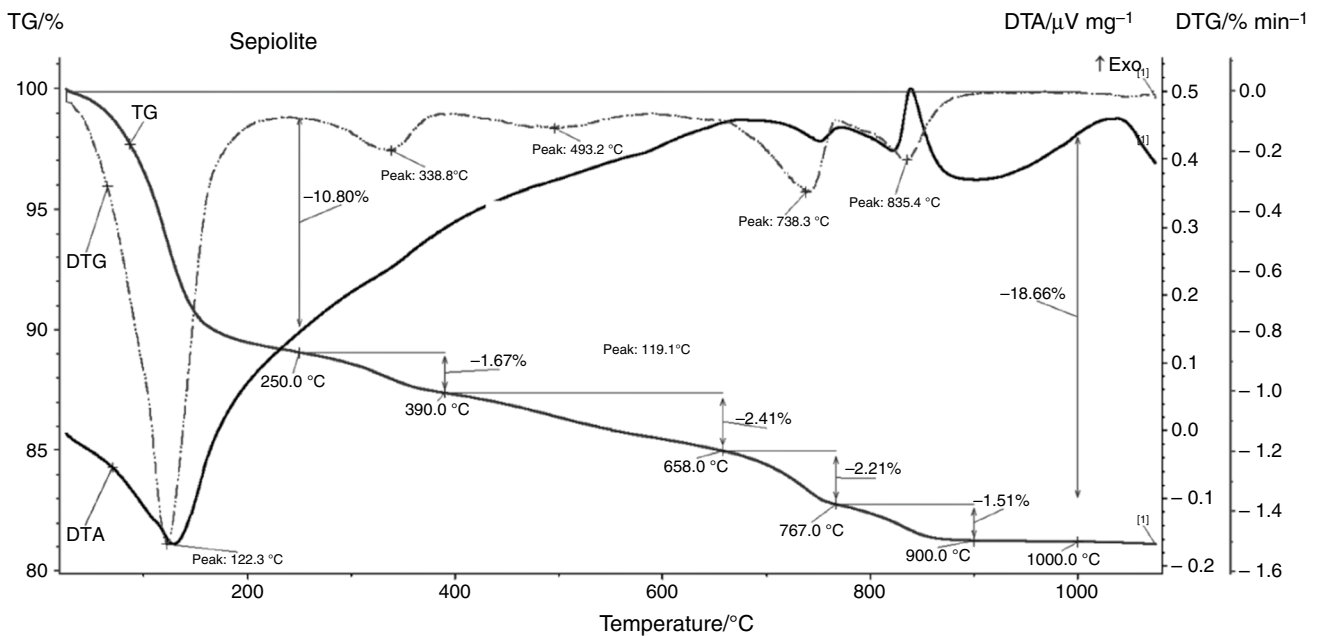**Fig. 3** DTA, TG and DTG curves of commercial (non-heat treated) attapulgite

Fig. 4 DTA, TG and DTG curves of commercial (non-heat treated) sepiolite

addition to the diffraction peaks of the main phase, there are also the peaks of calcite and quartz (Fig. 1). Sepiolite gives diffraction peaks from the sepiolite, enstatite and calcite (Fig. 2). The presence of calcite and quartz in the attapulgite and sepiolite is not surprising, because these are typical components of sedimentary rock.

Thermal analysis (DTA/TG/DTG) of attapulgite and sepiolite samples

DTA/TG and DTG studies were performed to identify the thermal behavior of attapulgite and sepiolite samples at different temperatures, as shown in Figs. 3 and 4 respectively.

The DTA, TG and DTG curves of attapulgite are illustrated in Fig. 3. Four endothermic peaks are observed on the DTA curve of attapulgite. The first and main endothermic one between 30 and 185 °C with the maximum rate at 119.1 °C is due to the loss of water adsorbed on the outer surfaces and a part of water bound in the crystal structure [34]. A mass loss of 9.98% is observed for this effect. The second endothermic mass loss of 2.41% between 185 and 315 °C with the maximum rate at 248.5 °C is a consequence of the loss of all zeolitic water and a part of chemically bound water [35]. The third endothermic mass loss of 3.94% between 315 and 570 °C with the maximum rate at 446.5 °C is associated with dehydroxylation of attapulgite [36]. The fourth endothermic mass loss of 2.70% between 570 and 760 °C with the maximum rate at 720.7 °C results from the decarbonization of the calcite included in attapulgite. At temperature range 800–870 °C, the exothermic peak connected with the formation of enstatite ($Mg_2Si_2O_6$) [37] is not visible on the DTA curve of attapulgite.

Figure 4 presents the DTA, TG and DTG curves of sepiolite. There are five endothermic peaks on the DTA curve of sepiolite. Maximum of the first and main endothermic peak between 20 and 250 °C with a maximum rate at 122.3 °C is due both to the loss of water adsorbed on the outer surfaces and that of zeolitic water [34, 38]. The mass loss corresponding to this effect is 10.80%. The second endothermic mass loss of 1.67% between 250 and 390 °C with the maximum rate at 338.8 °C results from the loss of bound water. The third endothermic mass loss of 2.41% between 390 and 658 °C with a maximum rate at 493.2 °C is due to the loss of more strongly bound water. The fourth endothermic mass loss is complex with two overlapping mass loss steps observed between 658 and 767 °C and 767 and 900 °C with the maximum rates at 738.3 and 835.4 °C, and the mass losses for these steps are 2.21% and 1.51%, respectively. These endothermic peaks are attributed to mass loss through the decarbonization of the dolomite included in sepiolite and the dehydroxylation of sepiolite, respectively [34, 39]. With the second step of dehydroxylation, the crystallization of enstatite also occurs, which corresponds to an exothermic peak at about 839 °C [35, 37].

Thermal activation of attapulgite and sepiolite samples

Thermal activation temperatures of the attapulgite and sepiolite samples were chosen on the basis of the results of the differential thermal analysis (DTA) and thermogravimetric (TG) tests of these materials. The heat treatment was done at temperatures slightly below the temperature of dehydroxylation.

For attapulgite, activation was carried out at temperatures of 650, 700 and 750 °C, that is, at temperatures at which dehydroxylation of attapulgite had already occurred. Temperatures of 650 and 750 °C were assumed to correspond to the temperatures of beginning and end of the decarbonization of calcite included in the attapulgite, respectively. The samples studied were denoted: A650, A700 and A750, where the number means the temperature of thermal activation.

For sepiolite, activation was carried out at temperatures of 800, 825 and 850 °C, and the samples were signified S800, S825 and S850, respectively. The temperature of 825 °C corresponds to the decomposition of sepiolite and the beginning of crystallization of enstatite [34, 39]. Temperatures of 800 and 850 °C were assumed to correspond to the temperatures of: the decarbonization of dolomite included in the sepiolite and further dehydroxylation of sepiolite with the transformation of sepiolite into enstatite [35, 37].

Verification of phase transformation during heat treatment of samples using the XRD method

The XRD patterns of thermally activated attapulgite and sepiolite samples are shown in Figs. 5 and 6, respectively.

As one can see in Fig. 5, heating to a temperature of 315 °C, that is, the temperature that refers to the first stage of dehydration, does not change the phase composition of the attapulgite sample. However, the decrease in the line intensity in the areas corresponding to the main peaks of saponite (001) and (111) (2θ $Cu_{K\alpha}$ equal to 6.2 and 34.7°2θ respectively) means the presence of low-crystalline forms of this mineral in the original (non-heated) attapulgite sample. Proper dehydration of the attapulgite sample (represented by the XRD pattern of sample heated at 550 °C) is combined with a clearly visible disappearance of the intensity of the main peak (110) at 8.7°2θ $Cu_{K\alpha}$ and the decrease in the distance between the layers of the packets after removal of water. Further heating to the temperature of 550 °C causes that the new intermediate phases are already visible: forsterite and early forms of enstatite (clino- and later proto-enstatite). Decomposition of the attapulgite and phase changes are accompanied by the release of excess silica. The next heating stage involves the decomposition of carbonate admixtures, and thus the oxides formed on this occasion react before the temperature of 750 °C with the activated silicates (released silica). Products of this reaction are magnesium silicates doped with Ca ions (diopside—$(Mg,Ca)SiO_3$) or Fe ions (forsterite—$(Mg, Fe)_2SiO_4$); it is assumed that silica consumption in this process will reduce the pozzolanic reactivity of activated attapulgite. The final products of the thermal treatment, beyond the thermal activation range (temperature of 950 °C), are well-crystallized silicates such as enstatite ($Mg_2Si_2O_6$), diopside and forsterite, without intermediate phase residues corresponding to the reactivity of the material toward calcium hydroxide (Fig. 5).
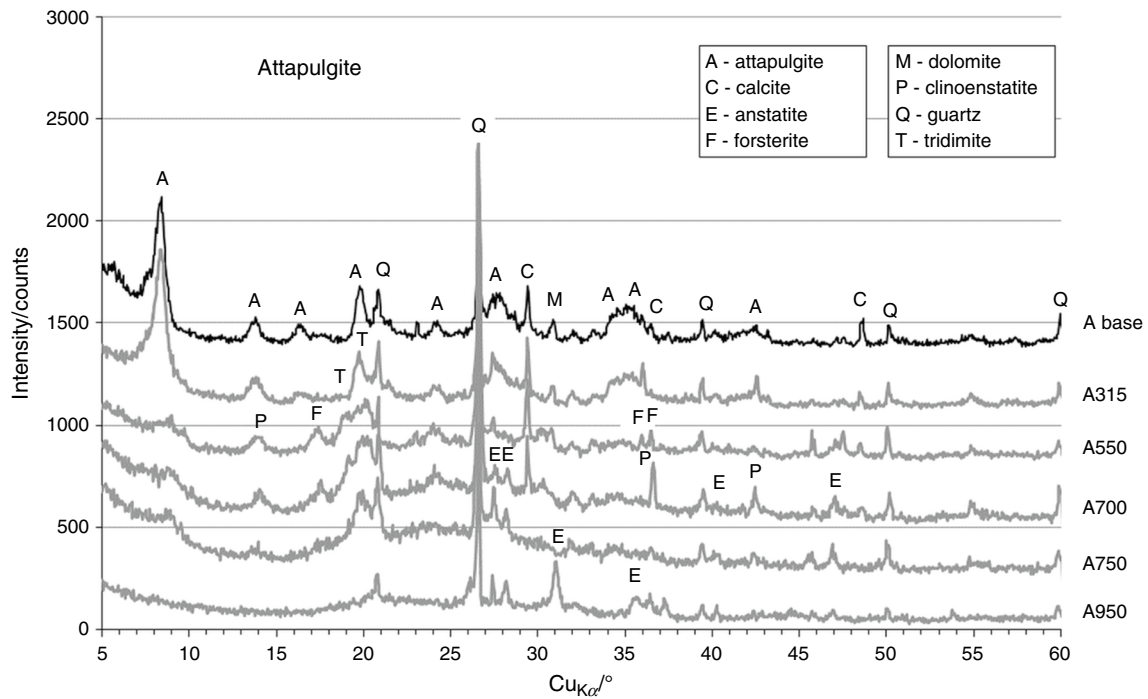
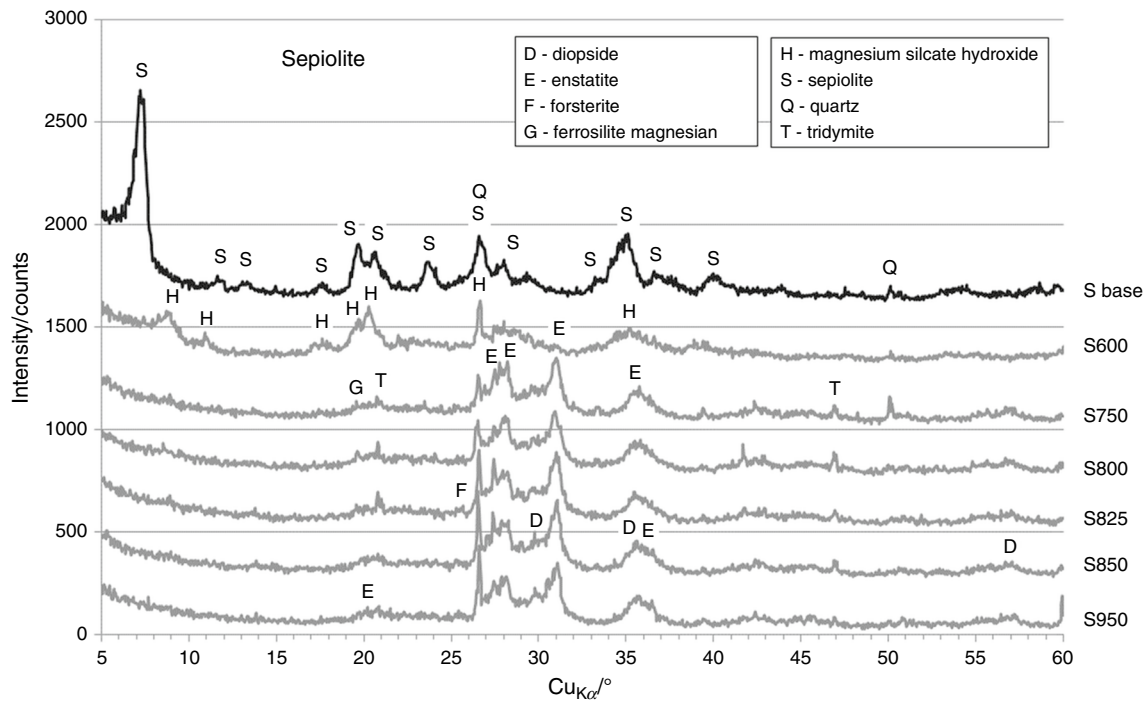**Fig. 5** XRD patterns of thermally activated attapulgite

Fig. 6 XRD patterns of thermally activated sepiolite

The phase transformation of sepiolite during heat treatment is similar to that of attapulgite; however, it should be noted that it differs by the temperature of the phase transformation and by the types of intermediate products (hydrated and non-hydrated magnesium silicate hydroxides) of the decomposition of sepiolite (Fig. 6). The diffraction

peaks of both the phases formed during the dehydration of sepiolite and the excess silica released are found in different positions in the XRD pattern in comparison with that of attapulgite. The main difference from the point of view of the planned use of the heat-treated material is a very narrow (compared to attapulgite) interval between the dehydroxylation temperatures and the formation of stable crystalline phases; the reduced availability of the decomposition products of sepiolite results in an increased proportion of the intermediate products of iron-magnesium silicate (magnesian ferrosilite). Final product of the heating of sepiolite is, as before, the mixture of silicate phases, but dominated by enstatite (Fig. 6).

Effect of thermal activation temperature on the content of pozzolanic reactive SiO_2 and Al_2O_3 in attapulgite and sepiolite samples: ASTM C379-65 standard [27]

The summary contents of pozzolanic reactive SiO_2 and Al_2O_3 according to the ASTM C379-65 standard [27] in thermally activated attapulgite and sepiolite samples are listed in Table 4.

The results of pozzolanic properties tests (Table 4) confirm that thermally activated attapulgite and sepiolite samples contain a large amount of reactive SiO_2 (Table 4). It is the result of progress in the transformation of basic magnesium silicate hydroxide into enstatite phases with the release of excess silica due to reactions:

- for attapulgite: $MgSi_4O_{10}(OH) \cdot 4H_2O \rightarrow MgSiO_3 + 3SiO_2 + H_2O\uparrow$
- for sepiolite: $Mg_4Si_6O_{15}(OH)_2 \cdot 6H_2O \rightarrow 4MgSiO_3 + 2SiO_2 + H_2O\uparrow$

As it is shown in Table 4, the A750 sample contains 29.17 and 3.26 mass% of reactive SiO_2 and Al_2O_3 (respectively) and the differences approach about 45 and 20% (respectively) compared to the one in the A650 sample. The S850 sample represents 16.80 mass% of reactive SiO_2 with a difference of approximately 8% compared to the S800 sample, while the content of reactive Al_2O_3 is only 0.88 mass% and is three times higher compared to the S800 sample.

Amount of $Ca(OH)_2$ consumed by thermally activated attapulgite and sepiolite samples according to the modified Chapelle test

The results of the $Ca(OH)_2$ consumption according to the modified Chapelle test are given in Table 5. The correct determination of $Ca(OH)_2$ consumed by the pozzolanic material using the Chapelle method [28] is when the value of 56 V/2 ratio (where the V means the volume of 0.1 N HCl necessary to titrate of the final solution obtained without tested material) is greater than 1000. In the case of the studied activated attapulgite and sepiolite samples, the value of 56 V/2 ratio is 1,005.

The results in Table 5 show that the attapulgite activated at higher temperature binds a higher amount of $Ca(OH)_2$ in its pozzolanic reaction. For the A650 sample, the amount of consumed $Ca(OH)_2$ is 754.58 mg and is comparable to that for A700 sample, which is 761.94 mg. In the case of the A750 sample, the amount of bounded $Ca(OH)_2$ increases to 765.62 mg, which means an amount higher by approximately 1.5% compared to the A650 sample.

For the sepiolite samples, the higher temperature of thermal activation the lower amount of $Ca(OH)_2$ consumed in the pozzolanic reaction (Table 5). The S825

Table 4 Summary contents of pozzolanic reactive SiO_2 and Al_2O_3 in thermally activated attapulgite and sepiolite samples determined according to the ASTM C379-65 standard [27]

Sample[a]	Reactive SiO_2 (mass%)	Reactive Al_2O_3	Summary
A650	20.05	2.61	22.66
A700	25.39	2.87	28.26
A750	29.17	3.26	32.43
S800	15.52	0.23	15.75
S825	15.92	0.70	16.62
S850	16.80	0.88	17.68

[a]Letter A or S is the attapulgite or sepiolite sample and the number next to letter A or S is the thermal activation temperature of these materials

Table 5 Content of $Ca(OH)_2$ consumed by thermally activated attapulgite and sepiolite samples determined according to the modified Chapelle test

Sample[a]	$Ca(OH)_2$ consumed by sample/mg	
	PAA[b]	PAS[b]
Blank test	–	–
A650	754.58	–
A700	761.94	–
A750	765.62	–
S800	–	552.13
S825	–	541.09
S850	–	537.41

[a]Letter A or S is the attapulgite or sepiolite sample and the number next to letter A or S is the thermal activation temperature of these materials

[b]PAA or PAS are a pozzolanic activity index of attapulgite and sepiolite, respectively
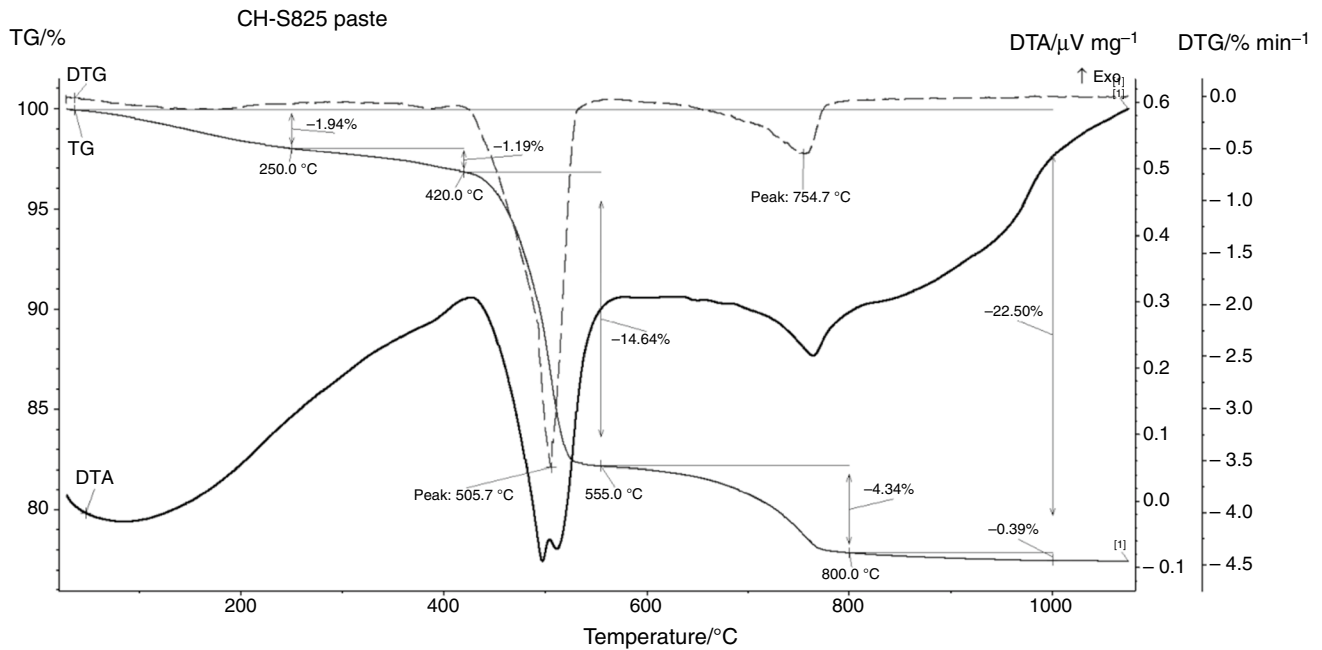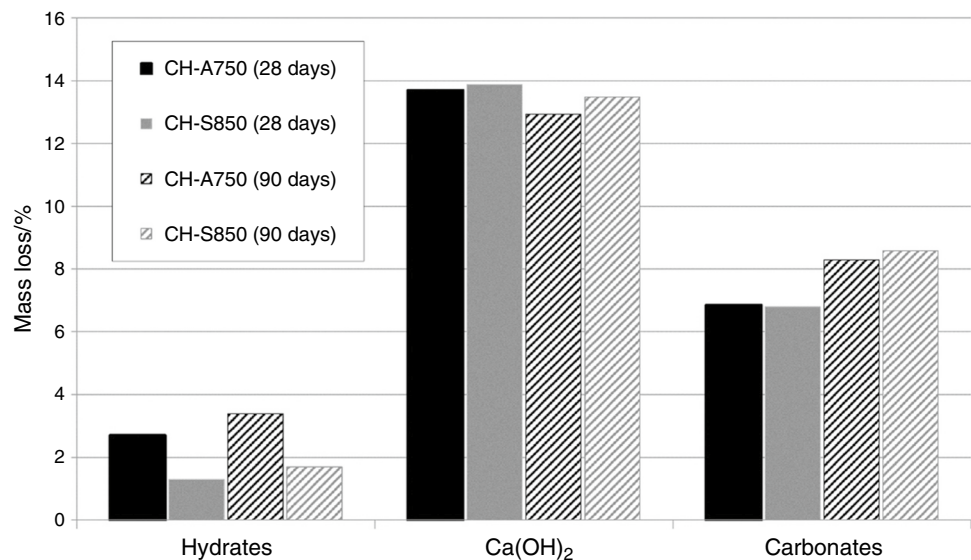
Fig. 7 DTA, TG and DTG curves of the CH-S825 paste (for further interpretation of the results of thermal analysis of the CH-A750 and CH-S850 pastes)

Fig. 8 TG losses of the pastes CH-A750 and CH-S850 heated beyond the temperature of 250 °C (dehydration of hydrates), from 550 to 850 °C (decarbonization of $CaCO_3$)

and S800 samples bind 541.09 and 537.41 mg of $Ca(OH)_2$ (respectively) and the differences approach about 2 and 3% (respectively) compared to the S800 sample, for which the amount of consumed $Ca(OH)_2$ is 552.13 mg.

When interpreting the results of the Chapelle test, it should be taken into account that they may be distorted by the content of Ca ions released from the thermal decomposition of carbonates in the attapulgite and sepiolite samples.

Determination of the amount of products formed in $Ca(OH)_2$-thermally activated additive-water system according to DTA/TG/DTG analysis

TG losses of pastes prepared from activated attapulgite (or activated sepiolite), $Ca(OH)_2$ and water—previously stored in tightly closed containers for 28 and 90 days at a temperature of 80 °C—are recorded. From the exemplary DTA/TG/DTG analysis of paste made of the $Ca(OH)_2$ and

S825 sample—named by the CH-S825 symbol (Fig. 7)—the following TG peaks were found: up to temperature of 250 °C (dehydration of hydrates), from 250 to 550 °C (dehydroxylation of $Ca(OH)_2$), from 550 to 850 °C (decarbonization of $CaCO_3$). The results for the CH-A750 and CH-S850 samples are presented in Fig. 8.

In the presented study, the effect of thermally activated additive (attapulgite or sepiolite) is most clearly manifested as an increase in the content of hydrates (the water contained in hydrates) in the pastes (Fig. 8). The results show a higher content of hydrates and progress of the pozzolanic reaction in the CH-A750 paste. According to the dominant $Ca(OH)_2$ content in the pastes studied, its consumption in the pozzolanic reaction can also be observed; however, it can also be observed that it is higher for the CH-A750 paste (higher TG losses in the temperature range of 250 to 550 °C). The influence of the A750 or S850 samples on the carbonization process is not observed (even for both additions used in the study).

Conclusions

1. During the thermal activation process, the attapulgite and sepiolite samples pass through the amorphization stage, where, before final crystallization, they show a higher pozzolanic reactivity.
2. After heating, both attapulgite and sepiolite transform to enstatite, and due to the presence of impurities, magnesium calcium iron silicates are also observed.
3. The main difference between attapulgite and sepiolite is the transition effect between dehydroxylation and crystallization, with a wide gap for attapulgite, whereas for sepiolite these effects overlap.
4. Increasing the activation temperature produces an increase in the content of pozzolanic reactive components (SiO_2 and Al_2O_3) in activated attapulgite and sepiolite and the resulting higher amount of $Ca(OH)_2$ consumed in the pozzolanic reaction of these materials. Despite the concerns, there is no loss of pozzolanic reactivity at the temperature of the reaction of silicates with accompanying phases.
5. In chemical methods, the activated attapulgite samples studied reveal a content of reactive pozzolanic reactive SiO_2 and Al_2O_3 that is comparable to that of metakaolinite.
6. Consumption of $Ca(OH)_2$ by forming pozzolanic reaction products is higher for the calcium hydroxide paste containing activated attapulgite samples, which should be reflected in the higher compressive strength of cement and lime mortars.
7. The research results allow to sort the existing findings known from the literature, pointing to the possibility of using higher activation temperatures of attapulgite and sepiolite.

The results of the pozzolanic reactivity of thermally activated attapulgite and sepiolite are not the only property that will influence their role in pastes and mortars. The significant specific surface of these additives, by increasing the water demand, will impact the rheological properties, air entrainment and porosity. This will decide on the appropriate dose of these additives to cement that ensures the appropriate mechanical properties. The studies will continue by analyzing the influence of thermally activated attapulgite and sepiolite on the rheological properties and pore structure of cement paste that determine the strength of cement mortar.

References

1. Massazza F. Pozzolana and pozzolanic cements. In: Hewlett P, editor. Lea's chemistry of cement and concrete. 4th ed. London: Elsevier; 2003. p. 471–635.
2. La PV, Liotta L, Golewski GL. The role of pozzolanic activity of siliceous fly ash in the formation of the structure of sustainable cementitious composites. Sustain Chem. 2022;3:520–34.
3. Golewski GL, Szostak B. Strength and microstructure of composites with cement matrixes modified by fly ash and active seeds of C-S-H phase. Struct Eng Mech. 2022;82:543–56.
4. Amarnath Y, Rama Chandurdu C, Bhaskar DV. Influence of fly ash replacement on strength properties of cement mortar. Int J Eng Sci Technol. 2012;4:3657–65.
5. Ogawa K, Uchikawa H, Takemoto K. The mechanism of the hydration in the system C3S and pozzolan. Cem Concr Res. 1980;10:683–96.
6. Sakai E, Miyahara S, Ohsawa S, Lee SH, Daimon M. Hydration of fly ash cement. Cem Concr Res. 2005;35:1135–40.

7. Jatale A, Tiwari K, Khandelwal S. Effects on compressive strength when cement is partially replaced by fly-ash. OSR J Mech Civ Eng. 2013;5:34–43.

8. Dodson VH. Pozzolans and the pozzolanic reaction. In: Dodson VH, editor. Concrete admixtures. Boston: Springer; 1990. p. 159–201.

9. Ho DWS, Lewis RK. Effectiveness of fly ash for strength and durability of concrete. Cem Concr Res. 1985;15:793–800.

10. Payá J, Monzó J, Peris-Mora E, Borrachero MV, Tercero R, Pinillos C. Early-strength development of Portland cement mortars containing air classified fly ashes. Cem Concr Res. 1995;25:449–56.

11. Chindaprasirt P, Jaturapitakkul C, Sinsiri T. Effect of fly ash fineness on compressive strength and pore size of blended cement paste. Cem Concr Compos. 2005;27:425–8.

12. Erdoğdu K, Türker P. Effects of fly ash particle size on strength of Portland cement fly ash mortars. Cem Concr Res. 1998;28:1217–22.

13. Payá J, Borrachero V, Peris-Mora E, Aliaga A, Monzó J. Improvement of Portland cement/fly ash mortars strength using classified fly ashes. Stud Environ Sci. 1994;60:563–70.

14. Tkaczewska E, Kłosek-Wawrzyn E. Wpływ jonów fosforanowych PO43- na proces hydratacji cementu. Cement Wapno Beton. 2012;17:401–8.

15. Mansour MS, Abadlia MT, Jauberthie R, Messaoudene I. Metakaolin as a pozzolan for high-performance mortar. Cement Wapno Beton. 2012;17:102–8.

16. Ferraz E, Andrejkovičová S, Hajjaji W, Velosa AL, Silva AS, Rocha F. Pozzolanic activity of metakaolins by the French standard of the modified Chapelle test: a direct methodology. Acta Geodyn Geomater. 2015;12:289–98.

17. Al-Rawas AA, Wahid Hago A, Corcoran TC, Al-Ghafri KM. Properties of Omani artificial pozzolana (sarooj). Appl Clay Sci. 1998;13:275–92.

18. Regourd M. Characterization and activation of addition product. In: Proceedings of the 8th international congress on the chemistry of cement, vol 1. Rio de Janeiro; 1986. p. 199.

19. Zghair LAG, Hamad HH, Mohamad SA, Alhamd RKS. Evaluate the compressive strength of cement paste modified with high reactivity attapulgite and affected by curing temperature. Mater Today Proc. 2022;52:361–6.

20. Shi T, Liu Y, Zhang Y, Lan Y, Zhao Q, Zhao Y, et al. Calcined attapulgite clay as supplementary cementing material: thermal treatment, hydration activity and mechanical properties. Int J Concr Struct Mater. 2022;16:10. https://doi.org/10.1186/s40069-022-00499-8.

21. Zhang S, Fan Y, Shah SP. Study on early characteristics of nano-attapulgite clay hardened cement paste based on different dispersion methods. SSRN Electron J. 2022;35. https://www.ssrn.com/abstract=4117117. Cited 29 Jun 2022.

22. Kh A-N. Influence of the activated Qatari attapulgite clay admixture on the mechanical properties and hydration kinetics of ordinary Portland cement. Qatar Univ Sci J. 2001;21:23–35.

23. Canbaz M, Eryilmaz M. Effect of high temperature on sepiolite—hydraulic lime mortar. In: International conference on performance-based and life-cycle structural engineering. University of Queensland Library; 2016. p. 1051–9.

24. Zhang S, Fan Y, Shah SP. Study on early characteristics of nano-attapulgite clay hardened cement paste based on different dispersion methods. SSRN. 2022. https://doi.org/10.2139/ssrn.4117117. Accessed 23 May 2022.

25. PN-EN 196-2. Methods for cement testing—part 2: chemical analysis of cement, Warszawa. 2013.

26. Gobbo LA, Cincotto MA, Quarcioni VA. Comparison between wet chemical analysis and Rietveld method quantification in white cement samples. In: 12th international congress on the chemistry of cement (ICCC 2007), Montreal. 2007. p. Oral presentation, M2-02.5.

27. ASTM C379-65T. Specification for fly ash for use as a pozzolanic material with lime. American Society for Testing and Materials, Washington. 1965.

28. NF P18-513. Addition for concrete—metakaolin—specifications and conformity criteria. Association Française de Normalisation, La Plaine Saint-Denis. 2012 (**in French**).

29. PN-EN 197-1. Cement—part 1: composition, specifications and conformity criteria for common cements, Warszawa. 2012.

30. Garciá-Romero E, Suárez M. On the chemical composition of sepiolite and palygorskite. Clays Clay Miner Vol. 2010;58:1–20.

31. Cookson MD, Stirk PMR. Determination of uncombined lime in Portland cement: the ethylene glycol method. Ind Eng Chem Anal Ed. 2019;9:451–3.

32. Taylor HFW. Cement chemistry. 2nd ed. London: Thomas Telford; 1997.

33. Kurdowski W. Chemistry of cement and concrete. Warsaw: Polish Scientific Publishers PWN; 2010.

34. Frost RL, Ding Z. Controlled rate thermal analysis and differential scanning calorimetry of sepiolites and palygorskites. Thermochim Acta. 2003;397:119–28.

35. Koukakis P, Tsakiridis P, Ntziouni A, Kordatos K, Perraki M. Ttapulgite clay of the ventzia basin, western macedonia, greece, as template insynthesizing amorphous carbonnanotubes. Bull Geol Soc Greece. 2016;50:1895–902.

36. Boudriche L, Calvet R, Hamdi B, Balard H. Surface properties evolution of attapulgite by IGC analysis as a function of thermal treatment. Colloids Surf A. 2012;399:1–10.

37. Che C, Glotch TD, Bish DL, Michalski JR, Xu W. Spectroscopic study of the dehydration and/or dehydroxylation of phyllosilicate and zeolite minerals. J Geophys Res. 2011;116:E05007. https://doi.org/10.1029/2010JE003740.

38. Frost RL, Kristof J, Horvath E. Controlled rate thermal analysis of sepiolite. J Therm Anal Calorim. 2009;98:423–8.

39. Sarı Yılmaz M, Kalpaklı Y, Pişkin S. Thermal behavior and dehydroxylation kinetics of naturally occurring sepiolite and bentonite. J Therm Anal Calorim. 2013;114:1191–9. https://doi.org/10.1007/s10973-013-3152-x.